IEEE Access
Multidisciplinary | Rapid Review | Open Access Journal

Received 25 May 2023, accepted 6 June 2023, date of publication 9 June 2023, date of current version 16 June 2023.

Digital Object Identifier 10.1109/ACCESS.2023.3284692

RESEARCH ARTICLE

Incipient Fault Diagnosis for DC–DC Converter Based on Multi-Dimensional Feature Fusion

WENTING HAN[1], LONG CHENG[1], WENJING HAN[1], CHUNMIAO YU[1], ZENGYUAN YIN[2], ZHEYI HAO[1], AND JINGTAO ZHU[2]

[1]Space Engineering University, Beijing 101416, China
[2]Astronaut Center of China, Beijing 100094, China

Corresponding author: Long Cheng (49225312@qq.com)

This work was supported in part by the National Natural Science Foundation of China under Grant 12003078.

ABSTRACT To effectively recognize the incipient potential faults caused by degradation of multiple components in DC-DC converters, a fault diagnosis method that involves multi-dimensional feature fusion and sensitive feature extraction is proposed. Firstly, the time-domain statistical characteristics of fault and normal samples are extracted. The KL divergence and normalized kurtosis of intrinsic mode functions (IMFs) between them are calculated by empirical mode decomposition (EMD). In order to further improve the feature discrimination, a sensitive feature extraction method based on Mahalanobis distance (SFMD) is designed to screen out the key features. Finally, the sensitive features are used to construct the SA-LSSVM (Simulated annealing-Least squares support vector machine) model to realize the fault diagnosis. The accuracy of fault diagnosis in simulation and hardware experiment are 99.61% and 97.93% respectively. Compared with other fault diagnosis and feature selection methods, the proposed method still has higher accuracy and better engineering practicability.

INDEX TERMS DC-DC converter, incipient fault, SA-LSSVM.

I. INTRODUCTION

DC-DC converter is an important component of secondary power supply, which is widely used in aerospace, new energy, transportation, communication systems and other fields [1], [2]. The degradation of the overall performance of most circuits is due to failure of key components [3]. At present, the fault diagnosis methods for DC–DC converter mainly focus on the soft fault and hard fault. Some faults may be caused by the subtle parameter deviations of the components in the early stage. This type of fault is called the incipient fault in this paper. It means that the minimum parameter change of the component is within the tolerance range [4]. If not detected the incipient faults in time, it will gradually deteriorate and cause the abnormal work of DC-DC converter. Therefore, it is necessary to identify the potential faults of DC-DC converter in the early stage.

The associate editor coordinating the review of this manuscript and approving it for publication was Yu Wang.

The research on fault diagnosis of DC-DC converter can be divided into three categories. Firstly, the model-based methods need to know the exact mathematical model of the DC-DC converter. Alexandre et.al proposed a real-time FDI algorithm with an integrated fuzzy logic scheme for detecting sudden failure at unknown time [5]. In [6], the adaptive sliding mode observer was designed for fault detection. The expert system uses the rich knowledge base and the reasoning mechanism separation technology. Aiming at the onboard power system, the fault reasoning and location were resolved by means of fault mode analysis and fault tree in [7]. For the satellite power system, an expert system was proposed in [8].

With the emergence of integrated circuits, complex fault causes are difficult to be fully covered by expert knowledge. The data-driven methods can effectively solve this problem [9]. A deep transfer kernel extreme learning machine auto encoder (DKEA) model was designed to solve the problem of insufficient data in [10]. The uncorrelated multi-linear principal component analysis are used for fault diagnosis in [11]. In [12], the soft fault diagnosis method based on wavelet

TABLE 1. Comparison with the existing method.

Ref	Experimental object	Fault component	Minimum identifiable parameter deviation	Feature extraction	Algorithm
[15]	buck/boost	Capacitor, Inductor, Ron of MOSFET	C −5% ESR +5% L −5% RL +5% Ron +5%	Overlap calculation	SVDD
[20]	buck	Capacitor	C −4%	Optimal fractional wavelet transform	SVM
[14]	buck-boost	Capacitor	C −10%	EMPCA	SVM
[19]	boost	Capacitor	C −10%	1DCNN	LSTM
[18]	sepic	Capacitor, Inductor, Ron of MOSFET	C −20% ESR +25% L −20% RL +30% Ron +20%	Wavelet packet transformation	CSA-DBN
[12]	buck	Capacitor, Inductor	C −10% L −10%	wavelet transform	FCMNN
The proposed method	buck/boost	Capacitor, Inductor, Ron of MOSFET	C −5% ESR +5% L −5% RL +5% Ron +5%	SFMD	SA-LSSVM

transform and fuzzy cerebellar model neural networks (WT-FCMNN) was proposed. Expectation Maximization Principal Component Analysis (EMPCA) and SVM were applied to buck–boost converter in [13]. Yang and Yue [14] proposed a soft fault diagnosis method for DC-DC converter based on overlap evaluation. In [15], online anomaly detection by Gaussian process regression (GPR) and genetic algorithm (GA) was proposed. In addition, the deep learning methods can realize the end-to-end fault diagnosis. In [16],the multilayer multivalued neuron neural network with a complex QR decomposition was proposed. A novel optimization deep belief network (DBN) optimized by crow search algorithm (CSA)was presented in [17]. In [18], convolutional neural network (CNN) based on channel attention mechanism was proposed. A fault feature extraction method based on multi-scale CNN was designed in [19], which fused fault feature extracted from convolution kernels of different scales.

This paper proposes an incipient fault diagnosis method for DC-DC converter based on multi-dimensional feature fusion (MDFF). The principle of this method is as follows: Firstly, the paper calculates the output signals in the time domain. The KL divergence and normalized kurtosis of intrinsic mode functions (IMFs) between them are calculated by empirical mode decomposition (EMD). Then, the sensitive feature extraction method based on Mahalanobis distance (SFMD) is used to increase the feature differentiation and achieve the feature fusion. Finally, simulated annealing (SA) is used to optimize the hyperparameter and the fault diagnosis model is con-structed based on it. The simulation and hardware experimental results show the proposed method can efficiently identify the faults of buck converter in the early stage.

Compared with the state-of-the-art research in Table 1. Firstly, a few methods can identify the faults of the multiple key components at the same time, most of them are just capacitor. However, the proposed method can recognize capacitor, inductor and MOSFET simultaneously. Secondly, the faults in the other studies are mainly caused by the lager parameter deviations. The output changes caused by these failures are observable. However, some incipient faults are caused by subtle degradation of key components. These studies are difficult to extract the incipient faults, and their accuracy are not satisfactory. The minimum identifiable parameter deviations of the proposed methods are relatively smaller than most methods, which can be up to 5%. It can effectively identify more fault types and incipient faults in the early stage.

The innovative contributions are summarized as follows. Firstly, it can solve the potential incipient faults of multiple components in DC-DC converters. All diagnosis accuracy is higher than other feature selection and fault diagnosis methods. Secondly, a feature selection method based on Mahalanobis distance is designed to get sensitive features, which can increase the feature differentiation and achieve the feature fusion. Thirdly, it has good generalization ability, which is suitable for different DC-DC converters, such as buck converter, boost converter and buck converter with the memristive load. In addition, the hardware experimental results show that the method has good anti-noise ability, which is close to the engineering practice.

The remainder of this paper is as follows. The principle of fault diagnosis method is presented in Section II. Section III introduces the experiments and analysis. Section IV draws the conclusion of this paper.

II. MDFF METHOD FOR INCIPIENT FAULT DIAGNOSIS

The proposed incipient fault diagnosis method consists of three steps. First is the multi-dimensional feature fusion including the statistical features, EMD-KL divergence and kurtosis. The second is the SFMD method, which eliminates redundant features and retains key features. Finally, the SA-LSSVM fault diagnosis model is used to carry out secondary dimension reduction and realize the incipient fault diagnosis for DC-DC converter.

A. FAULT FEATURE EXTRACTION

1) FEATURE EXTRACTION BASED ON TIME DOMAIN

As time goes by, the change of the temperature, humidity and pressure of the circuit will lead to the degradation of key components, thus forming the incipient faults of

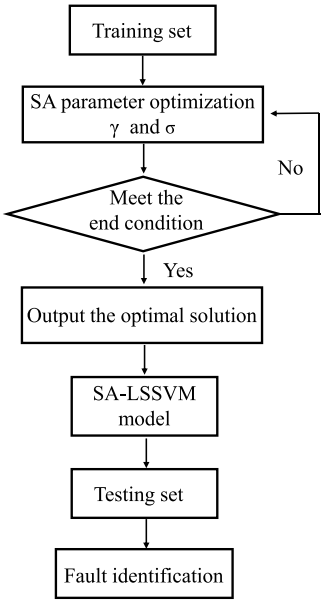

FIGURE 1. The process of SA-LSSVM.

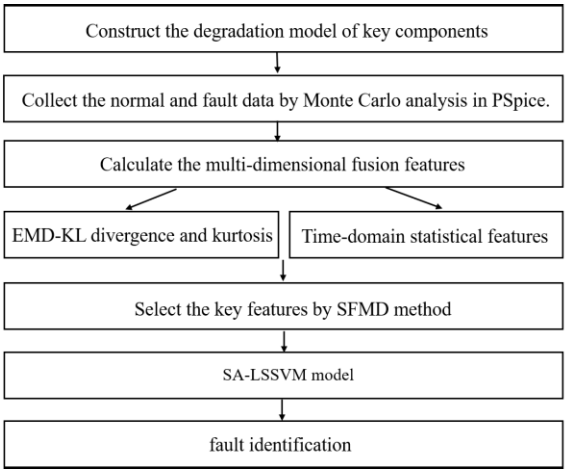

FIGURE 2. Procedure of fault diagnosis method.

DC-DC converter. Feature extraction based on statistical characteristics can directly reflect the change of the response. This paper calculates the six-dimensional statistical characteristics including mean, ripple voltage, RMS, variance, kurtosis and skewness, all of them are normalized. The $u = [u_1, u_2, \ldots, u_N]$ denotes the output response. The total number of sampling points is N.

Equation (1) expresses the mean m of output signal, which reflects the overall trend of the output response.

$$m = E(u) = \frac{1}{N}\sum_{i=1}^{N} u_i \tag{1}$$

The ripple voltage p refers to the change between the maximum and minimum values of the stable waveform, as expressed in (2). When the components degrade, the ripple varies linearly.

$$p = \max(u_i) - \min(u_i) \tag{2}$$

Equation (3) expresses the RMS c of the output signal.

$$c = \sqrt{\frac{1}{N}\sum_{i=1}^{N} u_i^2} \tag{3}$$

The variance v is used to measure the deviation between the sample and the mean, as expressed in (4).

$$v = \sqrt{E(u-m)^2} = \sqrt{\frac{1}{N-1}(\sum_{i=1}^{N} u_i^2 - N(E(u))^2)} \tag{4}$$

The larger the kurtosis is, the greater difference between the fault and the normal state, and it is defined as (5).

$$k = E(x^4) - 3[E(x^2)]^2 = \sqrt{\frac{1}{N}\sum_{i=1}^{N} u_i^4} \tag{5}$$

Equation (6) expresses the skewness s, which denotes the asymmetry of the output signal distribution.

$$s = E[(\frac{u-m}{v})^3] = (\frac{1}{N}\sum_{i=1}^{N} u_i^3)/\sqrt{\frac{1}{N}\sum_{i=1}^{N} u_i^2} \tag{6}$$

The time domain analysis of DC-DC converter is intuitive. Then statistical features of N_f samples are calculated and normalized respectively, which forms the original feature vectors F_s of $(6 \times N_f)$.

$$F_s = [m.p, c, v, k, s] \tag{7}$$

2) FEATURE EXTRACTION BASED ON EMD-KL DIVERGENCE

The statistical features can't fully reflect the circuit degradation information. The traditional signal processing method will cause that the fault features are not accurate. In this paper, IMFs are obtained by EMD of the output signal, and their KL divergence and normalized kurtosis are calculated to constitute fault feature vectors.

The principle of EMD is to make original signal relatively stationary. According to the local characteristic structure of the original signal $f(t)$, IMFs of single frequency and one residue $res(t)$ are decomposed from it, which realizes the multi-resolution analysis of DC-DC converter.

$$f(t) = \sum_{i=1}^{N} IMF_i(t) + res(t) \tag{8}$$

KL divergence $D(p||q)$ denotes the difference between two probability distributions, as expressed in (9).

$$D(p||q) = \int_{x\in X} p(x)\log\frac{p(x)}{q(x)} \tag{9}$$

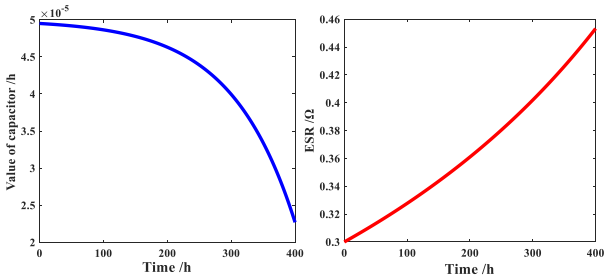

FIGURE 3. Electrolytic capacitor degradation model.

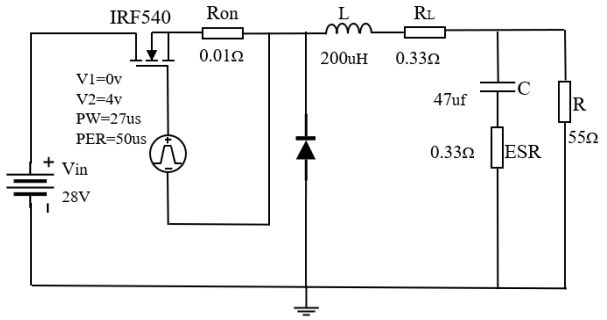

FIGURE 4. Schematic of buck converter.

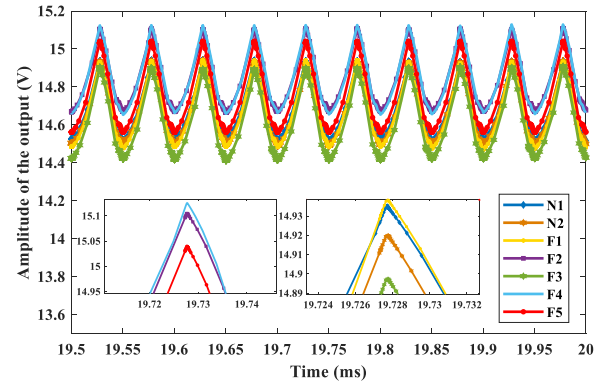

FIGURE 5. Output waveforms of N1-F5.

$p(x)$ and $q(x)$ are the probability density function of fault and normal sample for DC-DC converter respectively. By calculating KL divergence between them, faults be detected. Its steps are as follows:

Step 1: Calculate total energy of each IMF, as expressed in (10), where n is the length of the output signal.

$$E_t = \sum_{i=1}^{k} (IMF_n(i))^2 \quad i = 1, 2, \ldots, n \tag{10}$$

Step 2: Divide each IMF into m segments on average, and calculate the energy of each segment.

$$E_{\ln} = \sum_{i=l_1}^{l_2} (IMF_n(i))^2 \quad m = 6 \tag{11}$$

where l_1 and l_2 are starting and ending points of the segment.

TABLE 2. Fault classes of buck converter.

	Number of degrading parameters	Parameters	Parameters deviation ratio
N1	1	Ron	+5%
N2	1	ESR	+3%
		C	-2%
F1	1	ESR	+8%
		C	-10%
F2	2	RL	+5%
		L	-5%
		Ron	+10%
F3	2	ESR	+15%
		C	-12%
		Ron	+12%
F4	2	ESR	+8%
		C	-10%
		RL	+12%
		L	-5%
F5	3	ESR	+12%
		C	-9%
		RL	+12%
		L	-5%
		Ron	+15%
F6	1	ESR	short circuit

Step 3: Calculate energy distribution $p_f(k)$ of the signal by

$$p_f(k) = \frac{E_{\ln}}{E_t} \tag{12}$$

Then the KL divergence of IMFs between fault and normal signal can be expressed as:

$$KL = \sum_{k=1}^{m} p_f(k) \times \log \frac{p_f(k)}{p_n(k)} \tag{13}$$

where p_f and p_n refer to the probability distribution of IMFs of the fault and normal signal.

Step 4: Calculate the kurtosis k of IMFs and normalize the kurtosis and KL divergence respectively in order to use them to construct SA-LSSVM model for incipient fault diagnosis, which can simplify the computational complexity and improve the accuracy. The feature vectors F_e are defined as follows:

$$F_e = [\frac{KL_1}{\max\limits_i(KL)}, \ldots, \frac{KL_i}{\max\limits_i(KL)}, \frac{k_1}{\max\limits_i(k)}, \ldots, \frac{k_i}{\max\limits_i(k)}] \tag{14}$$

B. SENSITIVE FEATURE EXTRACTION BASED ON MAHALANOBIS DISTANCE (SFMD)

For the incipient fault diagnosis of DC-DC converter, extracting sensitive features from high-dimensional features is the premise to improve the diagnosis accuracy. The original feature vectors have a large amount of information, but the uncorrelated features increase the sample size. It leads to the curse of dimensionality and reduces the effectiveness of fault identification. To solve these problems, the paper proposes the SFMD method. Calculate the sensitive factors of the feature vectors to screen out the key features according to the corresponding threshold value.

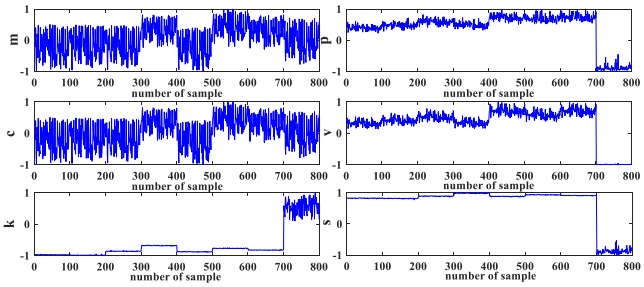

FIGURE 6. Time domain statistical characteristics.

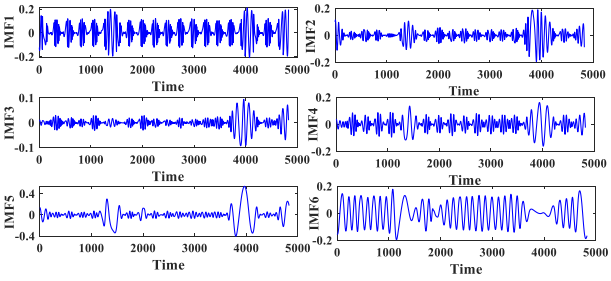

FIGURE 7. EMD decomposition results of N1.

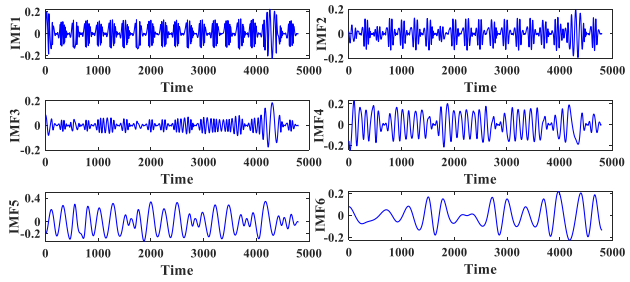

FIGURE 8. EMD decomposition results of F1.

TABLE 3. Energy distribution of IMFs of N1 and F1.

		IMF1	IMF2	IMF3	IMF4	IMF5	IMF6
N1	Pn1	0.1156	0.0835	0.0426	0.0777	0.0242	0.2091
	Pn2	0.2419	0.1155	0.0402	0.2342	0.2276	0.2020
	Pn3	0.0821	0.0414	0.0404	0.0763	0.0221	0.1142
	Pn4	0.1087	0.0421	0.0225	0.0913	0.0137	0.1866
	Pn5	0.1544	0.5105	0.5144	0.3286	0.5145	0.1044
	Pn6	0.2973	0.2070	0.3399	0.1919	0.1978	0.1837
F1	Pn1	0.1878	0.1024	0.0805	0.2232	0.1994	0.0431
	Pn2	0.1254	0.1647	0.0914	0.1541	0.1778	0.1159
	Pn3	0.1274	0.1143	0.0386	0.1873	0.1987	0.1026
	Pn4	0.1266	0.1519	0.1266	0.1468	0.1437	0.1797
	Pn5	0.1469	0.1716	0.1342	0.1375	0.1431	0.2045
	Pn6	0.2859	0.2952	0.5287	0.1511	0.1373	0.3542

Using the Mahalanobis distance (MD) to denote the covariance of the feature vectors, which can calculate the similarity between features. Compared with Euclidean distance, it is not limited by dimension, which can eliminate the correlation interference. The principle of SFMD is as follows: the features have a strong inter-class distinction between different fault samples and a good intra-class cohesion between similar fault samples. The steps of the proposed method are as follows:

Step 1: By multi-dimensional feature fusion of 6 dimensional statistical features and 12 dimensional EMD features,

TABLE 4. EMD feature vectors of F1.

Fault type	IMF	KL divergence	kurtosis	feature vectors
F1	IMF1	0.6489	0.9342	F= [0.6489,0.3659,
	IMF2	0.3659	0.1899	0.3784,0.3492,0.0199,
	IMF3	0.3784	0.4907	0.0171,0.9342,0.1899,
	IMF4	0.3492	0.1908	0.4907,0.1908,0.2045,
	IMF5	0.0199	0.2045	0.2737]
	IMF6	0.0171	0.2737	

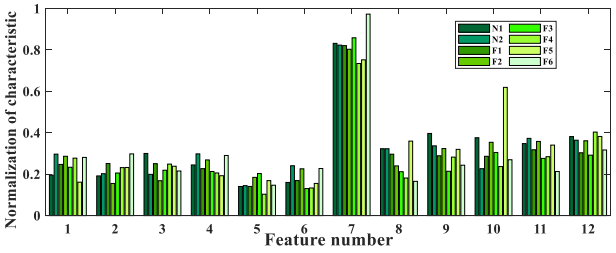

FIGURE 9. EMD-normalized characteristic parameter atlas.

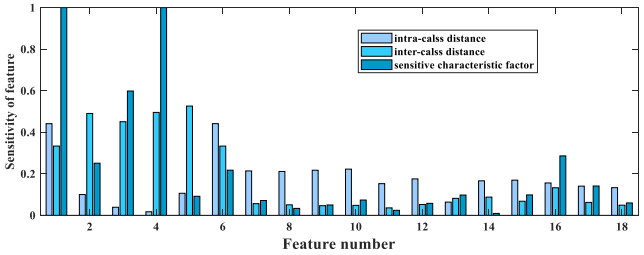

FIGURE 10. Results of SFMD in the ideal condition.

the 18-dimensional features F are shown as (15):

$$F = \{F_{i,j,l}, i = 1, 2 \ldots, N_f, \quad j = 1, 2 \ldots, M, l = 1, 2, \ldots, L\} \tag{15}$$

where N_f, M and L denote the 800 samples, 8 fault types, and 18 features respectively.

Step 2: Calculate the mean MD within the class d_l^{in} for each feature by:

$$d_l^{in} = \frac{1}{M} \sum_{j=1}^{M} \frac{1}{N \times (N-1)} \times \sum_{\substack{i=1 \\ n \neq i}}^{N} (md(F_{i,j,l} - F_{n,j,l})) \tag{16}$$

$$md(F_{i,j,l}, F_{n,j,l}) = \sqrt{(F_{i,j,l} - F_{n,j,l})^T \sum^{-1} (F_{i,j,l} - F_{n,j,l})} \tag{17}$$

Then calculate the weight ratio V_l^{in} of the intra-class distance of 8 faults by:

$$V_l^{in} = \frac{\max(d_l^{in})}{\min(d_l^{in})} \tag{18}$$

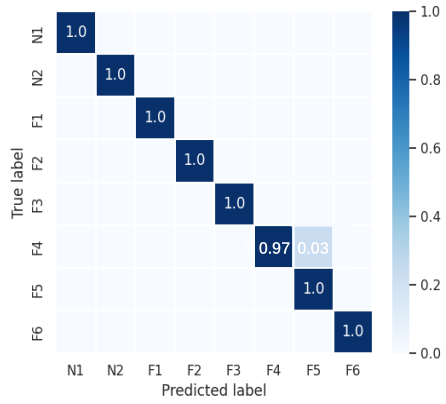

FIGURE 11. The confusion matrix in the simulation experiment.

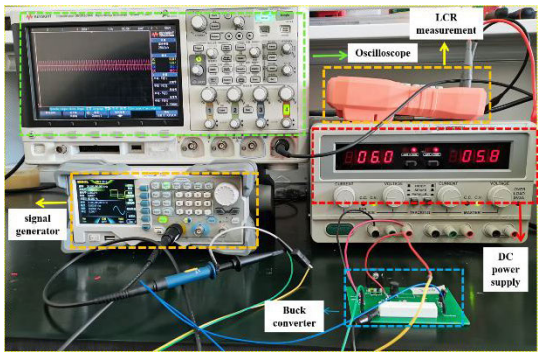

FIGURE 12. Hardware experiment platform.

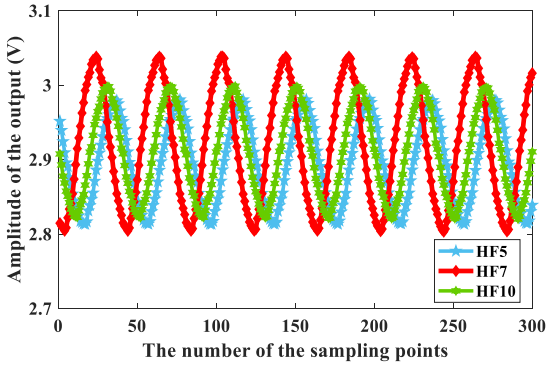

FIGURE 13. Waveforms of the fault states HF5 HF7 HF10 in the hardware experiment.

Step 3: Calculate the mean MD between classes d_l^{bet} for each feature by:

$$d_l^{bet} = \frac{1}{M \times (M-1)} \sum_{\substack{i=1 \\ i \neq n}}^{M} (|m_{i,l} - m_{n,l}| \tag{19}$$

$$m_{i,l} = \frac{1}{N} \sum_{i=1}^{N} F_{i,j,l} \tag{20}$$

TABLE 5. Each characteristic sensitive factor in the ideal condition.

Time domain feature	mean	range	kurtosis
	1	0.2510	0.5985
	skewness	SD	valid value
	1	0.0918	0.2174
EMD, KL divergence	IMF1	IMF2	IMF3
	0.0714	0.0335	0.0498
	IMF4	IMF5	IMF6
	0.0737	0.0242	0.0577
EMD, kurtosis	IMF1	IMF2	IMF3
	0.0977	0.0092	0.0983
	IMF4	IMF5	IMF6
	0.2862	0.1412	0.0597

TABLE 6. Precision, Recall, and F1 in the simulation experiment.

Fault classes	Precision	Recall	F1	Accuracy
N1	1.0	1.0	1.0	1.0
N2	1.0	1.0	1.0	1.0
F1	1.0	1.0	1.0	1.0
F2	1.0	1.0	1.0	1.0
F3	1.0	1.0	1.0	1.0
F4	1.0	0.973	0.981	0.969
F5	0.962	1.0	0.985	1.0
F6	1.0	1.0	1.0	1.0

Then calculate the weight ratio V_l^{bet} of the inter-class distance of 8 faults by:

$$V_l^{bet} = \frac{\max(d_l^{bet})}{\min(d_l^{bet})} \tag{21}$$

Step 4: The sensitive feature factor s_l for each feature is calculated and normalized as follows, where θ is the scale factor.

$$s_l = \theta \times \frac{d_l^{bet}}{d_l^{in}} \quad s_l = \frac{s_l}{\max(s_l)} \tag{22}$$

$$\theta = \frac{1}{\frac{V_l^{in}}{\max(V_l^{in})} + \frac{V_l^{bet}}{\max(V_l^{bet})}} \tag{23}$$

If s_l is close to 1, the feature is more sensitive for DC-DC converter, which can effectively distinguish different incipient faults. If s_l is close to 0, the feature is less important, which is irrelevant to the circuit degradation.

The proposed method SFMD has two advantages: Firstly, the calculation is simple and time-consuming. For the incipient faults, the original features have poor recognition effect, but the selected features have a good distinction between subtle faults, which can avoid the overlap of features from the perspective of quantitative analysis. Secondly, when the data is obtained through Monte Carlo analysis, the parameter changes in the tolerance range will not affect the good cohesion of the features. The selected sensitive features can continuously and stably reflect the properties of the degraded converters.

C. FAULT DIAGNOSIS BASED ON SA-LSSVM

LSSVM is an extended algorithm of SVM, which is used to solve the optimal classification problem of nonlinear samples in high dimensional space and avoid the dimensional

disaster when training large samples. For the training set $S = \{(x_1, y_1), (x_2, y_2), \ldots, (x_n, y_n), \}$ and nonlinear mapping $\varphi(x)$, the optimal decision function of LSSVM is as follows:

$$y = \omega^T \cdot \varphi(x) + b \tag{24}$$

where ω *is* weight vector and b is constant.

According to the principle of risk minimization, the constraint problem is established:

$$\begin{cases} \min\limits_{\omega,e,b} \phi(\omega, e) = \dfrac{1}{2}\omega^T\omega + \dfrac{1}{2}\gamma \sum\limits_{k=1}^{N} e_k^2 \\ y_k = \omega^T \cdot \varphi(x_k) + b + e_k \end{cases} \tag{25}$$

where γ is regularization parameter, e_k is error.

Use Lagrange multiplier to solve the constraint problem, function estimation of LSSVM is as follows:

$$y(x) = \sum_{k=1}^{N} \alpha_k K(x, x_k) + b \tag{26}$$

where $K(x, x_k)$ is kernel function, such as Radial Basis function, Gaussian kernel and Linear kernel. The suitable kernel function can improve the performance of LSSVM.

In order to further improve the accuracy of fault diagnosis, SA algorithm is used for parameter optimization of LSSVM. The SA algorithm has strong global search ability. It simulates the annealing process to optimize the hyperparameters γ and σ in LSSVM. Firstly, set the current solution to its initial value and new solutions are obtained by cooling. Random search is conducted by the Metropolis criterion and the optimal solution of LSSVM is obtained by repeated sampling with decreasing temperature. The process of SA-LSSVM is shown in Fig.1.

D. PROCEDURE OF THE FAULT DIAGNOSIS

Step 1: Construct the degradation model of key components and determine the incipient faults. Collect the normal and fault samples by Monte Carlo analysis in PSpice.

Step 2: Calculate the multi-dimensional fusion features including the time-domain statistical characteristics and EMD-KL divergence and kurtosis.

Step 3: Calculate the sensitive feature factors and select the key features by the SFMD method.

Step 4: Train the SA-LSSVM fault diagnosis model by the sensitive features to realize the incipient fault diagnosis of DC-DC converter. The specific procedure of the proposed method is shown in Fig.2.

III. EXPERIMENTS AND ANALYSIS

The proposed method is used for incipient fault diagnosis of DC-DC converter. In order to verify the validity of it, the simulation and hardware experiments are carried out. The key components of DC-DC converter are electrolytic capacitor, inductor and MOSFET. Therefore, it is necessary to analyze the degradation mechanism of these components in DC-DC converter.

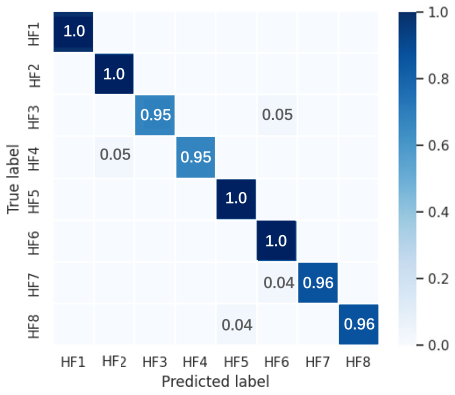

FIGURE 14. The confusion matrix in the hardware experiment.

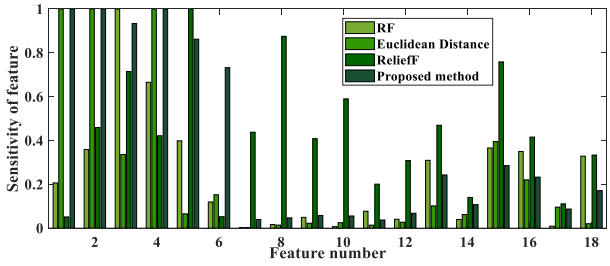

FIGURE 15. Sensitivity of features by different feature selection methods.

The electrolytic capacitor is used to realize energy storage and filter during voltage conversion. Its failure mechanism includes suddenness and gradualism. The equivalent circuit includes capacitor C and equivalent resistance R_C. Influenced by stress and environment, R_C and C will gradually increase and decreases respectively. The degradation model of electrolytic capacitor is shown as (27) and (28), and the degradation curve is shown in Fig.3.

$$ESR(t) = \frac{ESR(0)}{(1 - 5673 \cdot t \cdot \exp(\frac{-4700}{T+273}))} = \frac{ESR(0)}{1 - 0.00134t} \tag{27}$$

$$C(t) = C(0)[1 - 0.01(e^{0.01t} - 1)] \tag{28}$$

where R_C (0) and $C(0)$ refer to the nominal value of the R_C and C. T denotes the temperature.

The temperature of the coil increases overtime, which results in the decrease of the inductor value. The equivalent circuit of inductor includes L and equivalent resistance R_L, whose degradation model is shown as (29).

$$L(t) = L(0) - 0.031t \tag{29}$$

MOSFET switches on and off, which is controlled by the driving signal. MOSFET undertakes 30% power loss. The on-resistance of MOSFET is R_{on}, and $R_{on}(0)$ is the nominal value. Its degradation model is defined as (30).

$$Ron(\mathrm{t}) = Ron(0) + 0.0035 * (e^{0.00495t} - 1) \tag{30}$$

The buck converter is selected as the object of study, and its schematic is shown in Fig.4. The simulation circuit is built

TABLE 7. Soft fault set in the hardware experiment.

	Number of degrading parameters	Parameters	Values of the parameters
HF1	1	R_L	1.595 Ω
		L	0.985 mH
HF2	2	R_C	2.891 Ω
		C	4.223 μF
		R_L	1.018 mH
		L	1.572 Ω
HF3	2	R_C	1.479Ω
		C	4.313μF
		Ron	40.252mΩ
HF4	2	R_L	1.516 Ω
		L	0.991 mH
		Ron	39.451 mΩ
HF5	2	R_C	1.653 Ω
		C	3.923 μF
		Ron	41.752 mΩ
HF6	2	R_C	2.031 Ω
		C	4.103 μF
		R_L	1.050 mH
		L	1.516 Ω
HF7	2	R_C	2.153 Ω
		C	4.088 μF
		R_L	1.063 mH
		L	1.492 Ω
HF8	2	R_C	1.657 Ω
		C	3.491 μF
		Ron	42.792 mΩ

in PSpice. The MOSFET is IRF540, the diode is D1N5819. The DC signal source Vin is +28V, the period of PWM signal is set to 50 ηs, and the duty cycle is 54%. The tolerance of the components is set to 5%.

The component parameters of the buck converter are calculated as follows:

$$D = \frac{U_o}{U_i} = \frac{15}{28} = 53.57\% \tag{31}$$

where D refers to the duty cycle, U_o and U_i represent the input and output voltage respectively. The switching frequency $fs = 20kHz$.

$$R = \frac{U_o}{I_o} = \frac{15}{0.27} = 55\Omega \tag{32}$$

where R refers to the load resistance, and I_o denotes the output rated current.

$$L = \frac{(U_i - U_o) * D}{fs * dl} = 200\mu H \tag{33}$$

where L refers to the value of the inductor, and output current ripple $dl = 1.74$ A.

$$C = \frac{U_o * (1 - D)}{8 * fs^2 * Vpp * L} = 47\mu F \tag{34}$$

where C refers to the value of the capacitor, and output voltage ripple $V_{pp} = 0.23$ V.

According to the degradation model of components, the normal and fault sets are injected into the simulation circuit. The fault classes are shown as Table 2. The tolerance of the components is set to 5%. So the minimum identifiable parameter deviation of each faults is 5%. N1-N2 is the normal set of parameter variation within the tolerance, F1-F5 is the set of subtle incipient soft faults, and F6 is the hard fault.

TABLE 8. Precision, Recall, and F1 in the hardware experiment.

Fault classes	Precision	Recall	F1	Accuracy
HF1	1.0	1.0	1.0	1.0
HF2	0.960	1.0	0.982	1.0
HF3	1.0	0.951	0.980	0.955
HF4	1.0	0.955	0.981	0.955
HF5	0.951	1.0	0.972	1.0
HF6	0.932	1.0	0.961	1..0
HF7	1.0	0.962	0.980	0.964
HF8	1.0	0.960	0.981	0.960

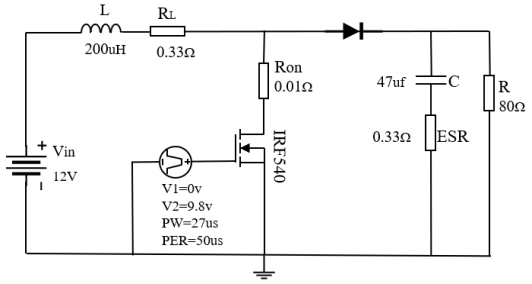

FIGURE 16. Schematic of boost converter.

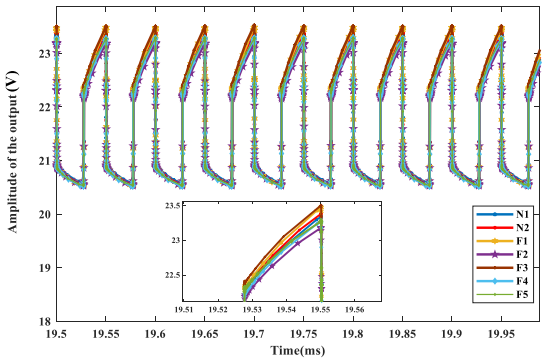

FIGURE 17. Output waveforms of boost converter.

Collect the stable output voltage for 19.5 *ms*-20 *ms*, the sampling interval is set to 0.5 ηs. The output waveforms of N1-F5 are given as Fig.5. It is difficult to identify the incipient soft faults because they have large overlap. 100 fault outputs of incipient faults are collected by Monte Carlo analysis.

A. DC-DC CONVERTER FAULT DIAGNOSIS

1) SIMULATION EXPERIMENT

The paper obtains the multi-dimension feature fusion, and the steps of fault feature extraction are as follows. In first, to realize rapid diagnosis, six time-domain features including the mean, the ripple voltage, the RMS, the variance, the kurtosis and the skewness of output voltage are calculated and normalized. The time-domain features of 800 samples are shown in Fig.6. 1-200 and 201-700 of each feature denote N1-N2 and F1-F5 respectively, and 701-800 denotes F6. Obtain IMF1-IMF6 of 800 samples by EMD method, which

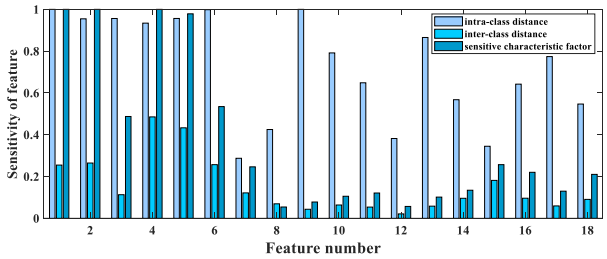

FIGURE 18. Results of SFMD for boost converter.

TABLE 9. Fault diagnosis accuracy by using different feature selection methods.

Fault classes	Proposed method, %	RF, %	Euclidean distance, %	Relief F, %
N1	100.00	82.6	90.90	77.30
N2	95.00	93.3	92.60	73.50
F1	96.60	76.9	90.00	76.90
F2	100.00	100	100.00	100.00
F3	100.00	90.00	78.30	75.00
F4	100.00	90.90	71.90	74.20
F5	100.00	92.30	63.30	57.10
F6	100.00	100.00	100.00	100.0
Average accuracy	99.00	91.00	84.50%	77.50

already contains abundant fault information to support the subsequent fault diagnosis.

The IMFs of N1 and F1 are shown in Fig.7 and Fig.8, which are obviously different. Each IMF is divided into 6 segments to obtain the energy probability distribution, as shown in Table 3. The KL divergence and kurtosis of IMFs in the same layer are calculated and normalized in order to use the SA-LSSVM model. The EMD-normalized characteristic parameter atlas are shown in Fig.9, which can effectively distinguish different kinds of faults. EMD fault feature vectors of F1 are shown in Table 4.

Combined the 18 features to form the multi-dimension features. Extract the sensitive features by the SFMD method, which use s_l to denote the sensitivity of features. The results of s_l of 18 features are shown in Table 5. The distributions of intra-class distance, inter-class distance and sensitive feature factors are shown in Fig.10. The horizontal axis represents 18 features. 1-6 represents time domain statistical features, 7-12 and 8-18 denote EMD-KL divergence and kurtosis. The mean value of sensitive factor $s_{lm} = 0.2312$. The features of $s_l > s_{lm}$ are left to form a 5- dimensional sensitive feature set. It can eliminate useless features and obtain better classification effect.

The configuration of the experimental platform is as follows: Windows10 64-bit operating system, CPU is i5-1135G7@2.40GHz, GPU is NVIDIA GeForce MX450. The program runs based on MATLAB. The fusion features of 800 data are randomly divided into training data and testing data by 3:1.The 600 samples are selected as the training set, 200 samples are used as the testing set. The training set is used to obtain the optimal SA-LSSVM model. The confusion matrix is used to represent the fault diagnosis results of the

TABLE 10. Fault diagnosis accuracy by using different diagnosis methods.

Fault classes	Proposed method, %	ELM %	LDA, %	SVM %	CNN
N1	100.00	89.50	81.00	59.60	80.00
N2	95.00	79.30	80.00	67.70	90.00
F1	96.60	77.40	81.80	63.20	95.50
F2	100.00	100.00	100.00	90.70	100.00
F3	100.00	96.20	96.80	81.70	92.50
F4	100.00	92.60	100.00	71.60	75.00
F5	100.00	96.00	83.30	55.90	75.00
F6	100.00	100.00	100.00	100.00	100.00
Average accuracy	99.00	90.50	91.00%	73.40	88.50%

TABLE 11. Computation complexity of different diagnosis methods.

	Proposed method	ELM	LDA	SVM	CNN
Iteration step	2	30	97	227	300
Run time (s)	0.745	0.912	0.849	4.652	8.502

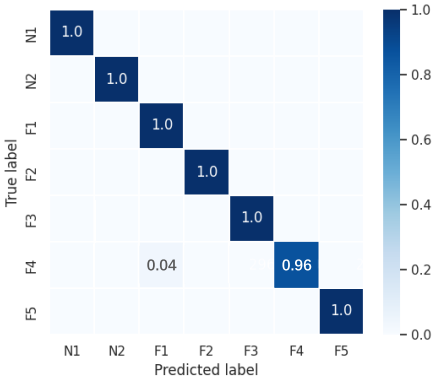

FIGURE 19. The confusion matrix of the boost converter.

buck converter. In the confusion matrix, columns represent the true fault labels obtained by SA-LSSVM, and rows represent the predicted fault labels. The value in each column shows the number of accurately predicted faults.

Confusion matrix has four basic indicators, namely TP (True Positive), FN (False Negative), FP (False Positive) and TN (True Negative). In this paper, the number of fault samples belonging to a certain type is positive, while the other is negative. The confusion matrix also has the secondary indicators, namely accuracy, precision, recall rate and F1. The equations of the indicators are as follows:

$$Accuracy = \frac{TP + TN}{TP + TN + FP + FN} \tag{35}$$

$$Precision = \frac{TP}{TP + FP} \tag{36}$$

$$Recall = \frac{TP}{TP + FN} \tag{37}$$

$$F1 = \frac{2 \times Precision \times Recall}{Precision + Recall} \tag{38}$$

The confusion matrix in the simulation experiment is presented in Fig.11. The accuracy, precision, recall, and F1 values of the proposed method are given in Table 6. As displayed

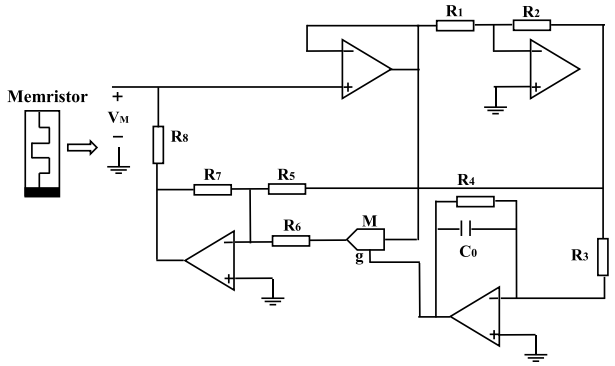

FIGURE 20. The simulator of the voltage-controlled memristor.

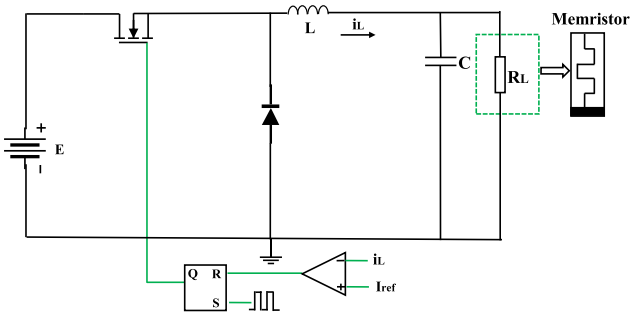

FIGURE 21. Schematic diagram of buck converter with memristor load.

TABLE 12. Each characteristic sensitive factor of boost converter.

Time domain feature	mean	range	kurtosis
	1	1	0.4874
	skewness	SD	valid value
	1	0.9785	0.5346
EMD, KL divergence	IMF1	IMF2	IMF3
	0.2463	0.0542	0.0781
	IMF4	IMF5	IMF6
	0.1056	0.1212	0.0570
EMD, kurtosis	IMF1	IMF2	IMF3
	0.1015	0.1345	0.2568
	IMF4	IMF5	IMF6
	0.2202	0.1299	0.2103

TABLE 13. Precision, Recall, and F1 of boost converter.

Fault classes	Precision	Recall	F1	Accuracy
N1	1.0	1.0	1.0	1.0
N2	1.0	1.0	1.0	1.0
F1	0.972	1.0	0.993	1.0
F2	1.0	1.0	1.0	1.0
F3	1.0	1.0	1.0	1.0
F4	1.0	0.963	0.982	0.963
F5	1.0	1.0	1.0	1.0

in Fig.11, in the F4 fault prediction, one sample is misjudged as F5. Other fault labels are classified correctly. The fault diagnosis accuracy of SA-LSSVM is 99.61%, which can realize the identification of incipient soft fault, hard fault of the buck converter.

2) HARDWARE EXPERIMENT

The hardware experiment is constructed to verify the effectiveness of the proposed method in the actual condition. The hardware platform involves the buck converter whose main components are the electrolytic capacitor, inductor and MOSFET. The C and R_C of electrolytic capacitor are 4.710 μF and 1.452 Ω. The L and R_L of the inductor are 1.071 mH and 1.423 Ω. The MOSFET is IRFP150 and Ron is 36 $m\Omega$. The DC power supply is +6 V. The frequency of the PWM signal is set to 20 kHz, and the duty cycle is set to 0.5 ms. Fig.12 shows the hardware platform.

Components with different values are selected to construct the soft fault of the hardware experiment. The soft fault of HF1-HF8 is shown in Table 7. 200 outputs of each fault are obtained from the actual circuit and the sampling interval is 1ms. From Fig.13, it can be seen that soft faults have obvious influence on the output.

Adopt the SFMD method to calculate the s_l of features in the hardware experiment. The mean value of sensitive factor $s_{lm} = 0.6293$. The features of $s_l > s_{lm}$ are left to form a 7-dimensional sensitive feature set. Then SA-LSSVM model is used to diagnose incipient faults. As displayed in Fig.14, there are some mistakes in the HF3, HF4, HF7 and HF8, and other fault labels are classified correctly. The fault diagnosis accuracy of SA-LSSVM is 97.93%, The accuracy, precision, recall, and F1 are given in Table 8. Due to the noise in the outputs of the hardware platform, the accuracy is lower than the simulation experiment, but it still meets the reliability requirements of the DC-DC converter.

B. COMPARISON OF DIFFERENT FEATURE SELECTION METHODS

In order to solve the problem of high dimension of original features in incipient faults of DC-DC converter, this paper proposes the SFMD method, which avoids dimension disaster and feature redundancy. To represent the superiority of this method, the comparison experiments are made with other feature selection methods including the Euclidean distance, Random Forest (RF) and Relief F methods. The method based on Euclidean distance means that the intra-class and inter-class distance is calculated by Euclidean distance, which is defined as (39).

$$\mathrm{E}d(F_{i,j,l}, F_{n,j,l}) = \sqrt{(F_{i,j,l} - F_{n,j,l})^2} \tag{39}$$

RF method calculates the average contribution of each feature in the random forest. The Gini index is used as an evaluation index to measure the contribution rate, which is defined as (40). Its score VIM of each feature is calculated respectively.

$$Gini(p) = 1 - \sum_{m=1}^{M} p_m^2 \tag{40}$$

where M and p_m indicate the number of fault classes and the weight of M.

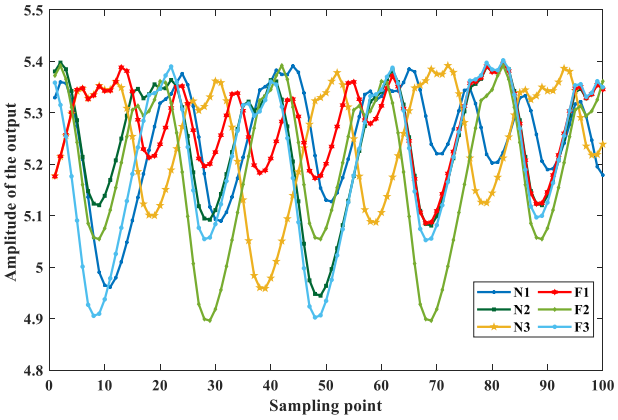

FIGURE 22. Output waveforms of buck converter with memristor load.

TABLE 14. Parameters of buck converter with memristor load.

Parameter	Value
E	8 V
L	0.3 mH
C	10 uF
C0	10 nF
R1, R2, R4, R5,R6, R7	10 kΩ
R3	40 kΩ
R8	1 Ω
f	20 kHz
g	1

The Relief F method randomly selects a sample R from the training data, and finds K nearest neighbor sample H from the same class. Find K nearest neighbor sample M from the different class, and updates the feature weight. The fault data with Gaussian noise from Section III-B are analyzed by Monte Carlo for 100 times to obtain the original features. The sensitivity of features by the four feature selection methods is shown in Fig.15. The fault diagnosis results by using different feature selection methods are shown in Table 9 combined with SA-LSSVM.

The SFMD method still has a higher average accuracy of 99.00%, which is 8.0%, 15.5% and 22.5% higher than RF, Euclidean distance and Relief F, respectively. The Euclidean distance method calculate the inter-class distance simply, but it is related to the unit of the index, and ignore

the influence of the total variation on the distance. The Relief F method is limited by finding nearest samples, which is not suitable for the multi-label classification. The RF method is affected by the number of decision trees, the size of training samples and internal node division, which will interfere with fault diagnosis. Therefore, the other three feature selection methods can't extract sensitive features well for the incipient fault diagnosis of DC-DC converter.

C. COMPARISON WITH OTHER DIAGNOSIS METHODS

To further demonstrate the superiority of this method, it is compared with other fault diagnosis methods, including extreme learning machine (ELM), linear discriminant analysis (LDA) support vector machine (SVM) and convolutional

TABLE 15. Soft fault set in the buck converter with memristor load.

	Number of degrading parameters	Parameters	Parameters deviation ratio
N1	-	-	-
N2	1	L	-5%
N2	1	C	-5%
F1	1	C	-12%
F2	1	L	-15%
F3	2	C	-15%
		L	-10%

TABLE 16. Precision, Recall, and F1 of the buck converter with memristor load.

Fault classes	Precision	Recall	F1	Accuracy
N1	1.0	1.0	1.0	1.0
N2	0.951	1.0	1.0	0.946
N3	1.0	1.0	0.991	1.0
F1	0.972	1.0	0.993	1.0
F2	1.0	1.0	1.0	1.0
F3	1.0	1.0	1.0	1.0

neural network (CNN). Use the noisy data from Section III-B, and the original features consist of time domain statistical characteristics, EMD-KL divergence and kurtosis. According to Table 2, the method proposed in this paper and the other four methods are used to construct diagnosis model. The results by using different fault diagnosis methods are shown in Table 10 combined with multi-dimensional feature fusion.

The proposed method still has a higher average accuracy of 99.00%, which is 8.5%, 8.0% 25.6% and 10.5% higher than ELM, LDA and SVM, CNN, respectively. The computation complexity of different diagnosis methods are shown in Table 11. The proposed method has the least iteration step and the least run time. Although the accuracy of ELM and LDA method are higher than 90%, their run time is longer than the SA-LSSVM method, and have more iteration steps. So the proposed method has the minimum computation complexity.

The reasons for the high accuracy of this method are as follows: LDA method depends on the data with large inter-class dispersion, which leads to the difficulty in identifying the categories with small inter-class dispersion. ELM belongs to the feedforward neural network, whose learning rate is difficult to determine. It is easy to fall into the local minimum dilemma and overtraining will also cause the performance of generalization decline. When SVM is faced with large data sets, the process of finding the optimal parameters will increase the time cost of fault diagnosis. CNN needs a lot of samples and the computation is heavy. In contrast, the SA-LSSVM method in this paper has the advantages of fast learning rate, high diagnosis accuracy and good robustness under the noisy condition.

D. EXPERIMENT OF DIFFERENT DC-DC CONVERTERS

To prove the proposed method is suitable for the incipient fault diagnosis of most DC-DC converters, the method is first applied to the boost converter, whose schematic is shown in Fig.16. The sampling time is set to 0.5 ηs, and the tolerance

of components is set to 5%. According to Table 2, the experiment is constructed in the ideal condition, and the output waveforms are given in Fig.17, whose overlap amplitude is less than 1V, which makes fault diagnosis more difficult. The time domain statistical features and EMD features are calculated. The results of the SFMD method and each characteristic sensitive factor for boost converter are given in Fig.18 and Table 12. Input the top 10 features into the SA-LSSVM. The accuracy, precision, recall, and F1 values of the boost converter are given in Table 13. As displayed in Fig.19, in the F4 fault prediction, two samples are misjudged as F1. Other fault labels are classified correctly. The accuracy of the proposed method is 99.47%, which demonstrates the proposed method is suitable for the other DC-DC converter. The fault diagnosis model has good portability and practicability.

The change in load type can indeed affect the nonlinear behavior of the DC-DC converter. In order to realize the stable and efficient operation of the system, it is important to study the dynamic characteristics of DC-DC converter under different power loads. As the fourth basic component, memristor has been widely used in engineering, biology, computer and other fields [25]. The memristor is used as the load of buck converter to verify the effectiveness of the proposed method [26].

Firstly, a voltage-controlled memristor simulator is constructed. Schematic diagram of voltage-controlled memristor simulator is shown in Fig.20. The nonlinear function model consists of an amplifier and a multiplier, which is shown in (41)-(42).

$$i_m = W(v_o)V_m = \frac{1}{R_8}(1 - \frac{R_7}{R_5} + \frac{R_7}{R_6}gv_o)V_m \tag{41}$$

$$\frac{dv_o}{dt} = \frac{V_m}{R_3C_0} - \frac{v_o}{R_4C_0} \tag{42}$$

where v_o denotes the voltage of C_0, i_m and v_m are the current and voltage of the memristor simulator.

Referring to Fig.21, the buck converter with the memristive load composes of a switch, a diode, an inductance, a capacitor, an RS flip-flop and a comparator. The buck converter with memristor load is built in PSIM and parameters are set as shown in Table 14. According to Table 15, the output waveforms of buck converter with the memristive load are shown in Fig.22. Apply the proposed method to it, the fault diagnosis accuracy can be up to 99.10%, which demonstrates the proposed method is suitable for DC-DC converter under different power loads. The accuracy, precision, recall, and F1 values of the buck converter with memristor load are given in Table 16.

IV. CONCLUSION

This paper presents an incipient fault diagnosis method based on multi-dimensional feature fusion of DC-DC converter. 1) The multi-dimensional features include the time domain statistics and EMD features. The SFMD method is proposed to obtain the sensitive features from the high dimensional information, which can realize the feature selection. 2) In the simulation and hardware experiments, all incipient fault states of different DC-DC converters can be diagnosed effectively. 3) Compared with the RF, Relief F and Euclidean distance method, the proposed SFMD method has better effect of feature selection. Moreover, the method has higher fault diagnosis accuracy and less time consuming than other diagnosis methods, such as LDA, SVM and ELM. 4) This method has good early warning ability for the incipient faults of DC-DC converter, which can effectively identify the weak degradation of components. It is also important for the health management and life cycle intelligent monitoring of switching power supply.

REFERENCES

[1] J. Falck, C. Felgemacher, A. Rojko, M. Liserre, and P. Zacharias, "Reliability of power electronic systems: An industry perspective," *IEEE Ind. Electron. Mag.*, vol. 12, no. 2, pp. 24–35, Jun. 2018.

[2] F. L. Tofoli, D. D. C. Pereira, W. J. de Paula, and D. D. S. O. Junior, "Survey on non-isolated high-voltage step-up DC–DC topologies based on the boost converter," *IET Power Electron.*, vol. 8, no. 10, pp. 2044–2057, Oct. 2015.

[3] S. Zhuo, A. Gaillard, L. Xu, C. Liu, D. Paire, and F. Gao, "An observer-based switch open-circuit fault diagnosis of DC–DC converter for fuel cell application," *IEEE Trans. Ind. Appl.*, vol. 56, no. 3, pp. 3159–3167, May 2020.

[4] Y. Yu, Y. Jiang, and X. Peng, "Multi-frequency test generation for incipient faults in analog circuits based on the aliasing measuring model," *IEEE Access*, vol. 6, pp. 34724–34735, 2018.

[5] A. M. Silveira and R. E. Araujo, "A new approach for the diagnosis of different types of faults in DC–DC power converters based on inversion method," *Electric Power Syst. Res.*, vol. 180, Mar. 2020, Art. no. 106103.

[6] Q. Su, Z. Wang, J. Xu, C. Li, and J. Li, "Fault detection for DC–DC converters using adaptive parameter identification," *J. Franklin Inst.*, vol. 359, no. 11, pp. 5778–5797, Jul. 2022.

[7] Z. Qin and G. Hong, "Big power system fault diagnosis expert system," *J. Beijing Univ. Aeronaut. Astronaut.*, vol. 33, no. 8, pp. 1026–1030, 2013.

[8] W. Ming, "Expert system of satellite power supply fault diagnosis based on CLIPS," M.S. thesis, Dept. Eng., Harbin Inst. Technol., Harbin, China,2017.

[9] K. Zhang, B. Gou, W. Xiong, and X. Feng, "An online diagnosis method for sensor intermittent fault based on data-driven model," *IEEE Trans. Power Electron.*, vol. 38, no. 3, pp. 2861–2865, Mar. 2023.

[10] J. Zhen and L. Zhen, "DC–DC buck circuit fault diagnosis with insufficient state data based on deep model and transfer strategy," *Exp. Syst. Appl.*, vol. 231, Mar. 2023, Art. no. 118918.

[11] Y. Fu, Z. Gao, and A. Zhang, "Data-driven parameter fault classification for a DC–DC buck converter," in *Proc. 6th Int. Symp. Environment-Friendly Energies Appl. (EFEA)*, Mar. 2021, pp. 1–7.

[12] Z. Han, Q. Lin, and Z. Zhang, "Soft fault diagnosis for DC–DC converters with wavelet transform and fuzzy cerebellar model neural networks," in *Proc. IEEE 9th Int. Power Electron. Motion Control Conf. (IPEMC-ECCE Asia)*, Nov. 2020, pp. 1811–1815.

[13] Y. Fu, Z. Gao, H. Wu, X. Yin, and A. Zhang, "Data-driven fault classification for non-inverting buck-boost DC–DC power converters based on expectation maximisation principal component analysis and support vector machine approaches," in *Proc. IEEE 1st Int. Power Electron. Appl. Symp. (PEAS)*, Nov. 2021, pp. 1–6.

[14] Y. Yu, Y. Jiang, Y. Liu, and X. Peng, "Incipient fault diagnosis method for DC–DC converters based on sensitive fault features," *IET Power Electron.*, vol. 13, no. 19, pp. 4646–4658, Dec. 2020.

[15] Y. Jiang, Y. Yu, and X. Peng, "Online anomaly detection in DC/DC converters by statistical feature estimation using GPR and GA," *IEEE Trans. Power Electron.*, vol. 35, no. 10, pp. 10945–10957, Oct. 2020.

[16] A. Luchetta, S. Manetti, M. C. Piccirilli, A. Reatti, F. Corti, M. Catelani, L. Ciani, and M. K. Kazimierczuk, "MLMVNNN for parameter fault detection in PWM DC–DC converters and its applications for buck and boost DC–DC converters," *IEEE Trans. Instrum. Meas.*, vol. 68, no. 2, pp. 439–449, Feb. 2019.

[17] Q. Sun, Y. Wang, and Y. Jiang, "A novel fault diagnostic approach for DC–DC converters based on CSA-DBN," *IEEE Access*, vol. 6, pp. 6273–6285, 2018.
[18] Y. Jiang, L. Xia, and J. Zhang, "A fault feature extraction method for DC–DC converters based on automatic hyperparameter-optimized 1-D convolution and long short-term memory neural networks," *IEEE J. Emerg. Sel. Topics Power Electron.*, vol. 10, no. 4, pp. 4703–4714, Aug. 2022.
[19] J. Yuan and W. Nian, "Fault diagnosis of buck converter under variable operating conditions based on optimal fractional wavelet transform," in *Proc. 11th Int. Conf. Prognostics Syst. Health Manag.*, Oct. 2020, pp. 286–290.
[20] W. Yi and W. You, "Characteristic parameters based on the degradation of the DC/DC converter fault prediction," *J. Instrum. Meters*, vol. 6, pp. 181–188, Jan. 2013.
[21] T. Gui, "P_DTW-LSTM fault prediction method for DC/DC circuits," *Electro Opt. Control*, vol. 26, no. 10, pp. 94–98, 2019.
[22] Y. Jiang, Y. Wang, Y. Wu, and Q. Sun, "Fault prognostic of electronics based on optimal multi-order particle filter," *Microelectron. Rel.*, vol. 62, pp. 167–177, Jul. 2016.
[23] J. Yue, Y. Yang, and P. Xi, "Multi-parameter identification of switching power supply based on key feature extraction and Elman neural network," *J. Electron. Meas. Instrum.*, vol. 35, no. 7, pp. 11–19, 2021.
[24] A. Sangswang and C. O. Nwankpa, "Noise characteristics of DC–DC boost converters: Experimental validation and performance evaluation," *IEEE Trans. Ind. Electron.*, vol. 51, no. 6, pp. 1297–1304, Dec. 2004.
[25] J. Sun, Y. Wang, P. Liu, S. Wen, and Y. Wang, "Memristor-based neural network circuit with multimode generalization and differentiation on Pavlov associative memory," *IEEE Trans. Cybern.*, vol. 53, no. 5, pp. 3351–3362, May 2023.
[26] B. Bao, N. Wang, Q. Xu, H. Wu, and Y. Hu, "A simple third-order memristive band pass filter chaotic circuit," *IEEE Trans. Circuits Syst. II, Exp. Briefs*, vol. 64, no. 8, pp. 977–981, Aug. 2017.

WENTING HAN was born in Shaanxi, China, in 1999. She received the B.S. degree from Space Engineering University, Beijing, China, in 2021, where she is currently pursuing the master's degree. Her research interests include aerospace launch, measurement technology, and digital and analog signal processing.

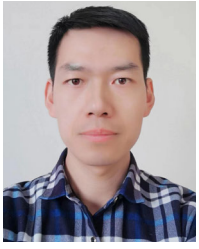

LONG CHENG was born in Gansu, China, in 1981. He received the B.S., M.S., and Ph.D. degrees from Space Engineering University, Beijing, China, in 2002, 2005, and 2008, respectively. He is currently a Professor with the Department of Astronautics Science and Technology, Space Engineering University. His research interests include aerospace launch and measurement technology.

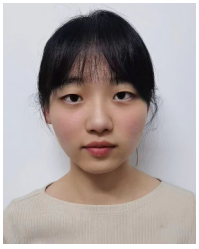

WENJING HAN was born in Shaanxi, China, in 1999. She received the B.S. degree from Space Engineering University, Beijing, China, in 2021, where she is currently pursuing the master's degree. Her research interests include aerospace launch, measurement technology, and spacecraft attitude control and measurement.

CHUNMIAO YU was born in Liaoning, China, in 1994. He received the B.S. degree from Beihang University, Beijing, China, in 2017, and the master's degree from Space Engineering University, Beijing, in 2019, where he is currently pursuing the Ph.D. degree. His research interests include the design and control of magnetically bearing, magnetic suspension inertial mechanism, and spacecraft attitude control and measurement.

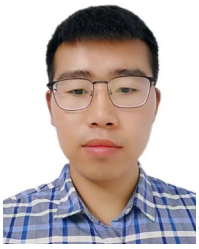

ZENGYUAN YIN was born in Henan, China, in 1993. He received the B.S. degree from the Shandong University of Technology, Zibo, China, in 2016, and the M.S. and Ph.D. degrees from Space Engineering University, Beijing, China, in 2018 and 2022, respectively. He is currently with the Astronaut Center of China, Beijing. His research interests include the design and control of magnetically bearing and magnetic suspension inertial mechanism.

ZHEYI HAO was born in Shanxi, China, in 2002. He is currently pursuing the B.S. degree with Space Engineering University, Beijing, China. His research interests include aerospace launch and measurement technology.

JINGTAO ZHU was born in Jiangxi, China, in 1970. He received the bachelor's degree from the Harbin Institute of Technology and the master's degree from the Beijing University of Aeronautics and Astronautics. He is currently with the Astronaut Center of China. He is also an Associate Researcher. His research interest includes biomedical engineering.